

**DYNAMIC FINITE ELEMENT MODELING OF THE EFFECTS OF SIZE ON THE UPPER SHELF ENERGY OF FERRITIC STEELS** - S. E. Sidener, A. S. Kumar, (University of Missouri), L. E. Schubert, M. L. Hamilton, (Pacific Northwest National Laboratory), and S. T. Rosinski (Electric Power Research Institute)

**SUMMARY**

Both the fusion and light water reactor programs require the use of subsize specimens to obtain sufficient irradiation data on neutron-induced embrittlement of ferritic steels. While the development of fusion-relevant size effects correlations can proceed analytically, it is more cost-effective at this time to use data currently being obtained on embrittlement of pressure vessel steels to test and expand the correlations developed earlier using fusion-relevant steels.

Dynamic finite element modeling of the fracture behavior of fatigue-precracked Charpy specimens was performed to determine the effect of single variable changes in ligament size, width, span, and thickness on the upper shelf energy. A method based on tensile fracture-strain was used for modeling crack initiation and propagation. It was found that the upper shelf energy of precracked specimens ( $USE_p$ ) is proportional to  $b^n$ , where  $b$  is ligament size and  $n$  varies from about 1.6 for subsize to 1.9 for full size specimens. The  $USE_p$  was found to be proportional to width according to  $W^{2.5}$ . The dependence on span was found to be nonlinear. The dependence on thickness was found to be linear for all cases studied. Some of the data from the FEM analysis were compared with experimental data and were found to be in reasonable agreement.

**PROGRESS AND STATUS**

Introduction

Subsize Charpy V-notch specimens have been proposed as a reasonable alternative to the ASTM standard full size Charpy specimens for the surveillance of nuclear reactor pressure vessels (RPV). The choice of subsize Charpy specimens would permit the placement of a sufficiently large number of specimens near the RPV for the purpose of monitoring its embrittlement throughout its lifetime. For example, if third size specimens were to be used, twenty seven specimens could be placed in the same volume as a single full size Charpy specimen. The choice of subsize specimens would not only increase the number of surveillance specimens that could be placed near the RPV, but it would also increase the uniformity of temperature and neutron fluence among the surveillance specimens. Furthermore, broken halves of irradiated full size specimens can be machined to fabricate subsize specimens which can be reinserted into the vessel for continued surveillance at higher fluences.

The choice of subsize surveillance specimens necessitates the development of methodologies for the prediction of the upper shelf energy of full size Charpy V-notch specimens based on subsize data. Numerous investigations have been carried out in the past to develop such methodologies [1-18]. These methodologies, however, are not applicable at all ductility levels of irradiated RPV materials. As the upper shelf energy (USE) diminishes from a high value (~200 J) to a low value (<100 J), three different methodologies have been found to be successful in correlating the USE of full and subsize specimens in different regimes of ductility.

The simplest of these methodologies is applicable at high ductility levels ( $USE > 200$  J). In this technique, normalized USE is defined as the ratio of the measured value and a normalization factor  $Bb^2$  [1,2] or  $(Bb)^{3/2}$  [3,4], often referred to as the fracture volume. The normalized values of USE are

equal for full and subsize Charpy specimens [1-4,7]. It is important to note that the normalization factor is independent of the span and the notch geometry, including the notch angle, notch depth, and the notch root radius. It is believed that blunting of the crack tip during macro-crack initiation and crack propagation makes the effects of span and notch geometry on USE minimal.

A little more complicated situation arises when the USE falls below 100 J. RPVs during the latter half of their life are expected to attain such low values of USE. Kumar and coworkers [5,6,8-10] have shown that the USE normalized by a factor equal to  $(Bb^2)/(S \cdot K_t')$  is equal for full and subsize specimens. Here  $S$  is span and  $K_t'$  is a modified stress concentration factor.  $K_t'$  is equal to the product of the elastic stress concentration factor at the notch root ( $K_t$ ), and the plastic constraint ( $Q$ ) [19].  $Q$  is equal to  $(1 + \pi/2 - \theta/2)$ , where  $\theta$  is the notch angle in radians. It is to be noted that at the low value of USE the blunting of the crack tip is relatively small and the effects of span and the stress concentration factor on crack initiation and propagation are significant.

For medium USE materials (USE ~ 150 J), there does not appear to be a clear consensus on the choice of a single normalization factor. For some materials, the normalization factor of Louden et al. [7] works well, while for some other materials, the normalization factors used by Corwin et al. [1,2] and Lucas et al. [5,6] work well [8].

Kumar et al. [15] have recently developed a methodology to correlate the USE of full size and subsize specimens for medium USE materials. This methodology is based on the partitioning of the USE into macro-crack initiation and crack propagation energies. The latter is approximated as the energy absorbed in the complete fracture of a specimen fatigue-precracked to half width ( $USE_p$ ). The macro-crack initiation energy ( $\Delta USE$ ) is approximated as the difference between the energy absorbed by a notched specimen USE and  $USE_p$ . The normalization factors for  $\Delta USE$  and  $USE_p$  were  $(Bb^2)/(S \cdot K_t')$  and  $(Bb^2)$ , respectively. The sums of the normalized values of  $\Delta USE$  and  $USE_p$  were found to be equal for full size and subsize specimens.

All of the size effects studies so far [1-18] have involved the use of specimens such that more than one variable (e.g. span, width, thickness, or notch geometry) changes from the full size to subsize specimens. Therefore, it is not possible to determine the dependence of USE on any of the geometry variables in an unambiguous manner.

The work presented in this paper was undertaken to elucidate the dependence of the upper shelf energy of precracked specimens ( $USE_p$ ) on single variables such as ligament size, width, thickness, and span. Precracked specimens were chosen since the absence of the notch eliminates the dependence of USE on  $K_t$ , the stress concentration factor, which, by itself, is a complicated function of the specimen dimensions and the notch geometry. Dynamic finite element modeling (FEM) using the computer code ABAQUS Explicit of the fracture of full (1.000 x 1.000 x 5.400 cm), half (0.500 x 0.500 x 2.360 cm), medium (0.400 x 0.400 x 2.360 cm) and third size (0.333 x 0.333 x 2.360 cm) specimens was performed. The  $USE_p$  determined by FEM was compared with the experimental data. For the full size Charpy specimen, the span was 4.600 cm. For all subsize specimens, the span was 2.000 cm. In addition, one set of half size specimens (0.500 x 0.500 cm) with full length of 5.400 cm and full span of 4.600 cm was also examined. For all five specimen geometries, four different precrack depths, i.e., 30%, 40%, 50%, and 60% of the full width ( $W$ ) of the corresponding specimen, were modeled. The experimental data for comparison were available for precrack depths that were 42%, 52% and 68% of  $W$ . A comparison was made between the experimental values and the best fit of the FEM data. A reasonable agreement was achieved in most cases. Having achieved the required confidence in the FEM analysis, a systematic study was performed to examine the dependence of  $USE_p$  on width ( $W$ ), thickness ( $B$ ), and span ( $S$ ).

### Experimental Procedure

The specimens used to obtain the experimental data were machined from A533B Plate 02 material. The material was obtained from Dr. R. K. Nanstad of Oak Ridge National Laboratory. The fatigue precracking and Charpy impact testing of the specimens were performed according to the procedures published earlier by Kumar et al. [15].

### Model Development

All modeling of the Charpy specimens and impact testing was conducted using a dynamic explicit-integration finite element code, ABAQUS Explicit, from the HKS corporation [20]. Two HP 9000-715/75 workstations were used to run the code. Depending on specimen geometry and mesh refinement, a typical simulation of the Charpy impact test could take from 3 to 40 hours of CPU time.

### Explicit dynamic analysis using ABAQUS

ABAQUS Explicit uses a dynamic analysis procedure which implements an explicit integration rule with the use of diagonal mass matrices [20]. The equations of motion are integrated using the explicit central difference integration rule:

$$\mathbf{j}^{i+\frac{1}{2}} = \mathbf{j}^{i-\frac{1}{2}} + \frac{\Delta t^{i+1} + \Delta t^i}{2} \bar{\mathbf{j}}^i$$

$$\mathbf{j}^{i+1} = \mathbf{j}^i + \Delta t^{i+1} \mathbf{j}^{i+\frac{1}{2}}$$

The superscript (i) refers to the increment number. The central difference integration is explicit in that the kinematic state may be advanced using known values of  $\mathbf{j}^{i-1/2}$  and  $\bar{\mathbf{j}}^i$  from the previous increment. In order to increase computational efficiency, ABAQUS uses diagonal element mass matrices. The accelerations at the beginning of the increment may be computed by:

$$\bar{\mathbf{j}} = \mathbf{M}^{-1} \mathbf{x} (\mathbf{F}^i - \mathbf{I}^i)$$

Where  $\mathbf{M}$  is the diagonal lumped mass matrix,  $\mathbf{F}$  is the applied load vector, and  $\mathbf{I}$  is the internal force vector. The code integrates through time using many small stable time increments. The time incrementation scheme in ABAQUS is fully automatic and requires no user intervention. The use of small increments (directed by the stability limit) is advantageous in that it allows the solution to proceed without iterations and without requiring tangent stiffness matrices. The explicit procedure is ideally suited for analyzing high speed dynamic events like those found in Charpy impact testing.

Assuming that the stable time increment does not change drastically during the analysis, the cost in CPU time for an explicit dynamic analysis is related to the size of the mesh in the following manner:

$$Cost \propto N \frac{T}{\Delta t}$$

where N is the total number of elements in the mesh, T is the duration of the event, and t is the stable time increment size. The stable time increment decreases exponentially with decreasing element size. Therefore, the total CPU cost usually increases linearly with the number of elements in the model, and exponentially with the refinement of the mesh.

#### ABAQUS failure model

ABAQUS Explicit contains an elastic-plastic material model which allows the modeling of crack growth by deleting elements from the mesh. ABAQUS treats crack initiation and growth by calculating a space-averaged strain and then deleting elements in the mesh when any element reaches an input-defined plastic failure strain ( $e_f^{pl}$ ). In order for this deletion of elements to produce stable results, the stress state of the damaged element must be reduced to zero by the time of failure. ABAQUS accomplishes this by applying a damage level to the material prior to failure. This damage parameter is used to degrade the stress state as well as the elastic moduli. The damage value of any element is zero until the strain in the element exceeds a user-defined offset failure strain ( $e_o^{pl}$ ). The damage in an element can range from zero (no damage) to one (failed) and is calculated from the equivalent plastic strain as follows:

$$DAMAGE = D = \frac{e^{pl} - e_o^{pl}}{e_f^{pl} - e_o^{pl}}$$

At each increment, the equivalent plastic strain ( $e^{pl}$ ) is obtained and damage is assessed using the above equation. Damage may not be removed from an element, and when the damage reaches a value of one, the element is deleted from the mesh and a crack is formed or extended.

#### User-defined material model

When modeling Charpy impact tests using the ABAQUS material failure model, a fundamental problem with the crack propagation is observed [21]. ABAQUS only determines the magnitude of plastic strain in an element relative to the failure criterion. This allows cracks to initiate and propagate under tensile or compressive constraints with identical failure criterion. In order to correct this problem, a user-defined Fortran subroutine is used to model the material constituent equations and hence model failure. This routine is called by ABAQUS instead of the normal material model. The routine uses the same mechanism for modeling crack initiation and propagation as the ABAQUS model with the exception of when the damage factor is incremented. A deviatoric stress given by

$$\sigma_{mean} = \frac{1}{3} (\sigma_{11} + \sigma_{22} + \sigma_{33})$$

is used to determine if an element is under tensile or compressive loading. If the value of  $\sigma_{mean}$  is positive then damage is allowed to increase in that increment. If  $\sigma_{mean}$  is negative or zero then no further damage can result. This user defined material failure model accurately models the fracture of a Charpy specimen under impact. The model has been tested and benchmarked against the ABAQUS Von Mises plasticity material model [21].

### Benchmarking

In order to obtain confidence in both the elastic response of the user defined material failure model and the ABAQUS finite element model which included initial and boundary conditions, a simple, low-velocity bar impact was modeled. Because an analytical solution for the maximum deflection in a simple bar is easily obtained, comparison of analytical and ABAQUS results would allow benchmarking of the model.

The analytical solution for a full size unnotched specimen under 3-point elastic impact loading was developed using a conservation of energy approach. If gravitational forces on the striker and bar are neglected, the kinetic energy of the striker prior to impact can be related to the strain energy stored in the elastically bent specimen. The maximum center load-line displacement (CLLD) of the bar can be given as a function of striker velocity. From small-displacement elastic theory, the displacement as a function of static load is given by:

$$\Delta = \frac{PL^3}{48EI}$$

where E is Young's modulus of the material and I is the moment of inertia of the specimen. The energy balance equation is written as:

$$U_k = U_e$$

$$\frac{1}{2}mv^2 = \frac{1}{2}P\Delta_{\max}$$

The above two equations are combined to give the maximum CLLD as a function of striker velocity,

$$\Delta_{\max} = \sqrt{\frac{mv^2 L^3}{48EI}}$$

The maximum displacement is linear with respect to striker velocity. The only assumptions used are that inertial effects in the bar are neglected, the striker is modeled as a rigid body, and the striker remains in contact with the specimen until maximum deflection is reached.

To simulate the elastic impact of a full size specimen, the striker was given a mass of 1 kg. The impact velocity of a rigid striker was varied from 10 cm/s to 150 cm/s and modeled using ABAQUS. A comparison of the results of maximum CLLD vs. striker impact velocity with the analytical elastic solution is given in Fig. 1. When the impact velocity reaches around 70 cm/s, the maximum stress in the bar at maximum CLLD exceeds the yield limit, thus moving into the plastic deformation regime. Before reaching this point, ABAQUS results agree with the elastic solution. As would be expected, the ABAQUS results diverge from the elastic solution as the impact velocity is increased beyond 70 cm/s.

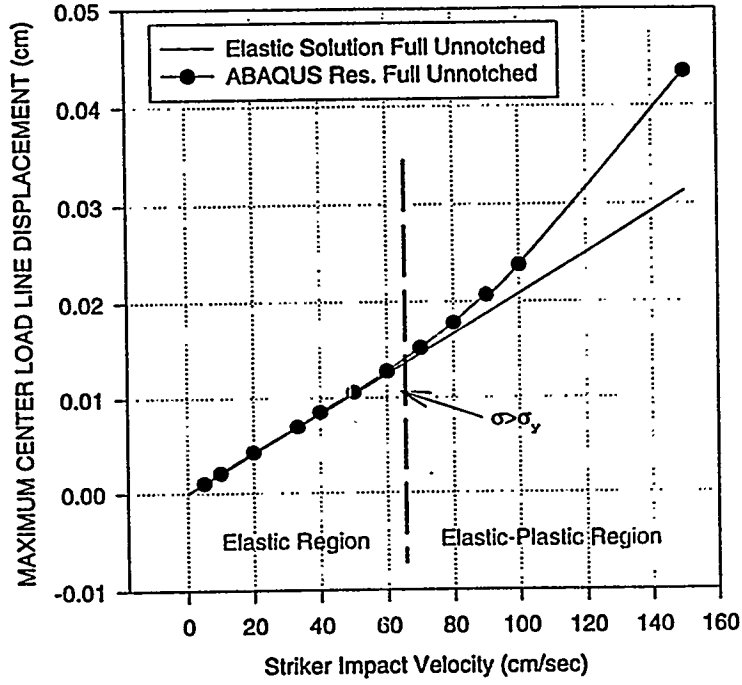


Fig. 1. Analytical Max. Load-Line Displacement Under Impact vs. ABAQUS Results

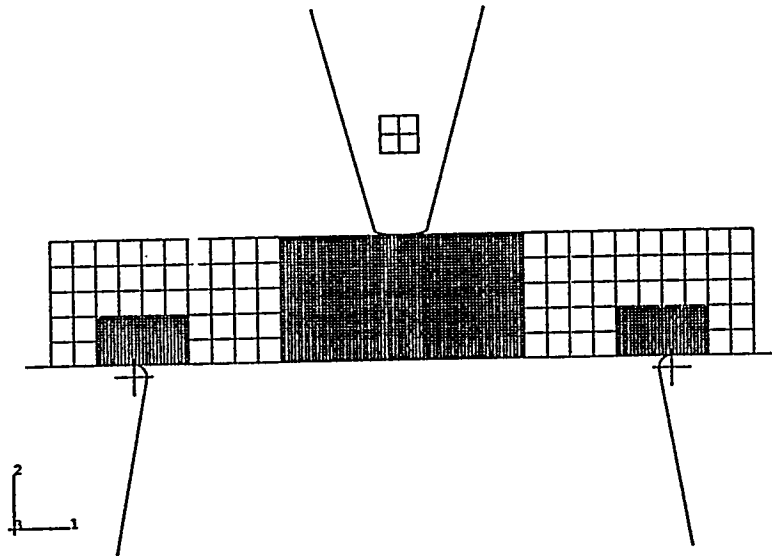


Fig. 2. 2D Finite Element Mesh

### Charpy impact modeling

A dynamic finite element model of the Charpy impact test was run in which fracture initiation and propagation to complete failure were considered. Both 2D half-symmetry and 3D quarter-symmetry models of the striker, precracked Charpy specimens, and anvil were constructed using the codes IDEAS-SDRC and ABAQUS. Models for full (1.000 x 1.000 x 5.400 cm), half (0.500 x 0.500 x 2.360 cm), half-2xL (0.500 x 0.500 x 5.400 cm), medium (0.400 x 0.400 x 2.360 cm), and third (0.333 x 0.333 x 2.360 cm) size specimens have been made for several USE materials. A study of finite element mesh schemes and coarseness was used to develop a stable and reliable model of the Charpy impact test [21]. The striker and anvils were modeled using rigid bodies. An illustration of the mesh for a full size specimen is given in Fig. 2. An area (or volume for 3D) around the crack plane has been refined as well as an area around the anvils. In order to save computing cost, the elements in the extremities of the specimen were left relatively coarse. The effect on USE of not refining the entire specimen is negligible. It was found that if the Charpy impact was modeled using conventional impact energies (around 200 J), the computational time was excessive. In order to speed up the simulation and therefore save CPU time, a high energy impact on the order of 80,000 J was used. Fig. 3 illustrates the effect of increasing the impact energy on the USE of a third size, medium USE specimen. It can be seen that with a difference of only 8.5% in USE, a savings of 69 hours of CPU time on an HP9000-715/75 can be made.

The material properties for A533B Plate 02 were obtained from the EPRI report (NP-933) Nuclear Pressure Vessel Steel Data Base [22]. Ramberg-Osgood constants for a true stress-strain curve were obtained from Haggag [23]. An initial bilinear stress-strain relation for A533B with a failure strain of around 30% was made. This 30% failure strain was chosen with the knowledge that the local failure strain would be higher than the EPRI 2 in. gauge length failure strain (~24%). The offset failure strain was then chosen at 10% less than the failure strain. It was found that the model becomes unstable if the difference between offset and failure strain is less than 5%. The USE of a full size specimen (precracked to 40% width) calculated by ABAQUS was compared to the corresponding experimental value of 35.5 J. The failure and offset strains were then shifted to calibrate the ABAQUS model with experimental data. It was found that the failure strain needed to be increased to 50%. This calibrated medium-USE material stress-strain curve is shown in Fig. 4.

### Results and discussion

Fig. 5 shows the upper shelf energy ( $USE_p$ ) of full size precracked Charpy specimens as a function of ligament size. The ABAQUS FEM material stress-strain curve was calibrated at a ligament size of 0.4 cm. The  $USE_p$  for three more ligament sizes (0.5, 0.6 and 0.7 cm) was then calculated using ABAQUS. A curve of the form  $USE_p = mb^n$  was fit through the four data points, where  $m$  and  $n$  are fitting parameters and  $b$  is the ligament size. The values of  $m$  and  $n$  were 202.0 and 1.90 for the best fit, with a correlation factor of 0.9992. It is worth noting that the value of  $n$  is quite close to 2. Fig. 5 also shows the experimentally obtained  $USE_p$  measurements for full size specimens with ligament sizes equal to 0.40, 0.48, and 0.64 cm. The scatter in the experimental data around the mean value is shown by a vertical band. The experimental data are in excellent agreement with the best fit curve.

Fig. 6 shows the calculated and experimental data for  $USE_p$  of half size specimens (0.500 x 0.500 x 2.360 cm). The best fit curve through the calculated data for  $USE_p$  of specimens with ligament sizes of 0.21, 0.26, 0.30, and 0.34 cm is represented by the equation  $USE_p = 57.0b^{1.55}$ . The first two experimental data points ( $b = 0.21$  and 0.26 cm) are in reasonable agreement but the third is substantially far away from the curve. Additional experiments and ABAQUS calculations are in progress to ascertain the reasons for this discrepancy. The discrepancy is particularly puzzling since

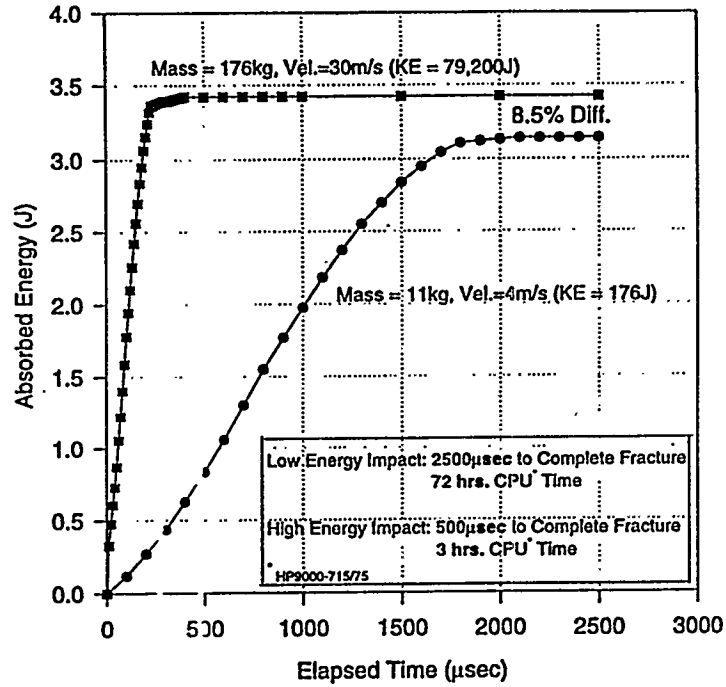


Fig. 3. Comparison of Low and High Energy Impact for 3D Third Size Medium USE Specimen (Precracked 50% W)

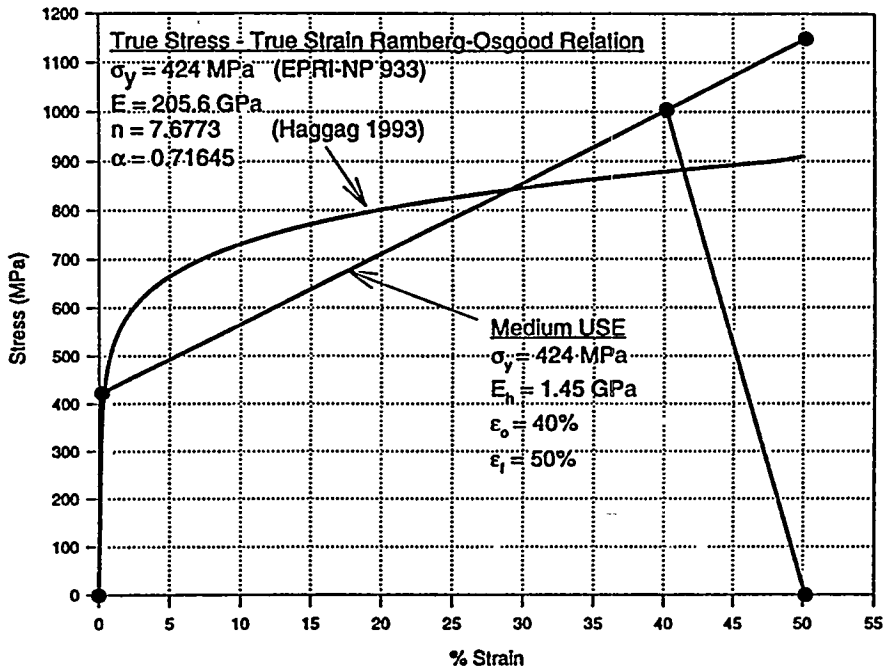


Fig. 4. Stress-Strain Curve of Medium USE for A533B Plate 02 Steel Used in ABAQUS

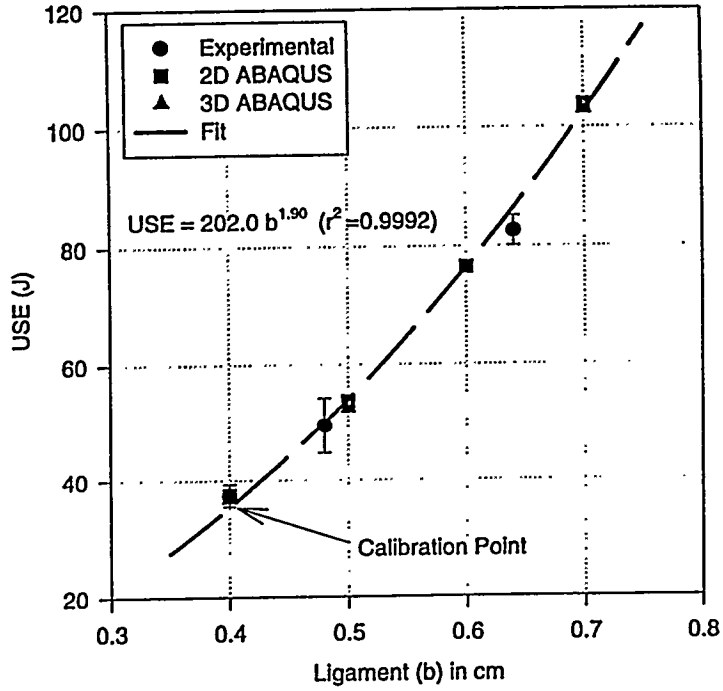


Fig. 5. USE vs. Ligament Size (b) for Full Size Medium USE Material

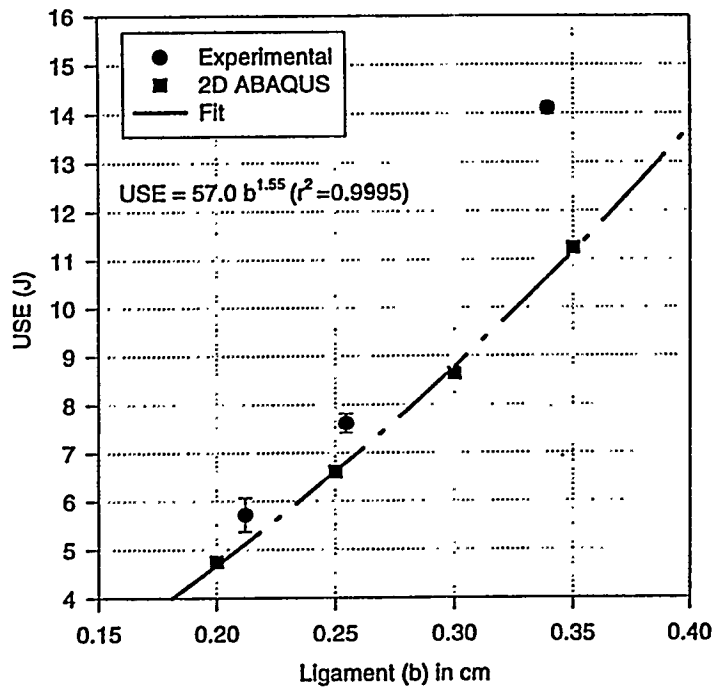


Fig. 6. USE vs. Ligament Size (b) for Half Size Medium USE Material

the ABAQUS calculations and experimental data are in excellent agreement for half size-2xL specimens (0.500 x 0.500 x 5.400 cm).

Fig. 7 shows the experimental and ABAQUS-calculated data for the half size full-length specimens. The calculated data can be best fit by the expression  $USE_p = 59.5 b^{1.53}$ . Fig. 8 shows the  $USE_p$  data for medium size specimens (0.400 x 0.400 x 2.360 cm). Both calculated and experimental data are shown. The calculated data can be best fit by the expression  $USE_p = 45.8b^{1.56}$ . The experimental data are in reasonable agreement. However, the difference between experimental and calculated data appears to increase with decreasing ligament size. The dependence of the  $USE_p$  on ligament size has decreased to approximately the 3/2 power for the subsize specimens (0.500 x 0.500 cm and 0.400 x 0.400 cm) from the roughly square dependence for full size specimens. Fig. 9 shows the dependence of the  $USE_p$  of third size (0.333 x 0.333 x 2.360 cm) specimens on ligament size. The computed values can be best fit by the expression  $USE_p = 44.8 b^{1.66}$ . The ligament size dependence of  $USE_p$  of third size specimens increased slightly from that of the half size specimens. The experimental values are consistently lower than the calculated data by about 5%.

From the foregoing analysis, it is quite clear that the ligament size dependence of full size and subsize specimens is not the same. There is a general tendency for the dependence to increase from an approximate value of 3/2 for subsize to about 2 for the full size specimens.

Having achieved good agreement between ABAQUS data and the experimental values, parametric studies were conducted to examine the width, span, and thickness dependence of  $USE_p$  using ABAQUS. The width (W) dependence of  $USE_p$  for full size specimens (50% precracked,  $b = 0.5$  cm) is shown in Fig. 10.  $USE_p$  is proportional to  $W^{2.51}$  for the ABAQUS calculated data.

The span dependence of the  $USE_p$  of full size specimens as shown in Fig. 11 is quite nonlinear. For specimens with spans ranging from 100% to 250% of standard full size specimens, the  $USE_p$  is almost independent of specimen size. However,  $USE_p$  rises steeply as the span decreases below 100% of the full size span. Under these conditions, it is difficult to assign a span dependence for  $USE_p$ .

The thickness (B) dependence of the full size  $USE_p$  has been found to be quite linear as shown in Fig. 12. In this figure, the thickness was allowed to vary between 30 and 120% of 1.0 cm (the full size standard thickness). This linear dependence is the reason why 2D and 3D calculations give results that are very close to each other, as shown in Fig. 5. A slight nonlinearity is seen, however, at lower values of thickness (~30%).

## CONCLUSIONS

The following conclusions were made regarding the impact energy of medium ductility materials (notched  $USE \sim 150$  J):

- (1) Dynamic finite element modeling by ABAQUS can be performed to predict the  $USE_p$  of full size precracked specimens based on subsize data. The required inputs are the stress-strain curve and the fracture strain of the material. Subsize data will serve as the calibration point.
- (2) Finite element modeling calculations of the  $USE_p$  were found to be in reasonable agreement with experimental data for full (1.000 x 1.000 x 5.400 cm), half (0.500 x 0.500 x 2.360 cm), half-2xL (0.500 x 0.500 x 5.400 cm), medium (0.400 x 0.400 x 2.360 cm) and third size (0.333 x 0.333 x 2.360 cm) specimens. The specimens were fatigue precracked so that ligament sizes (b) ranged from

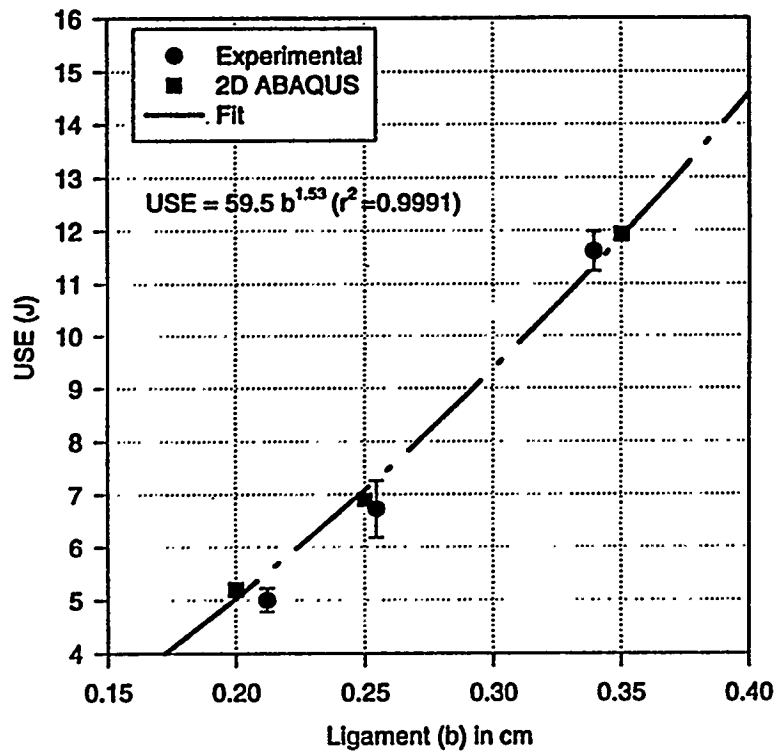


Fig. 7. USE vs. Ligament Size (b) for 2xL Half Size Medium USE Material

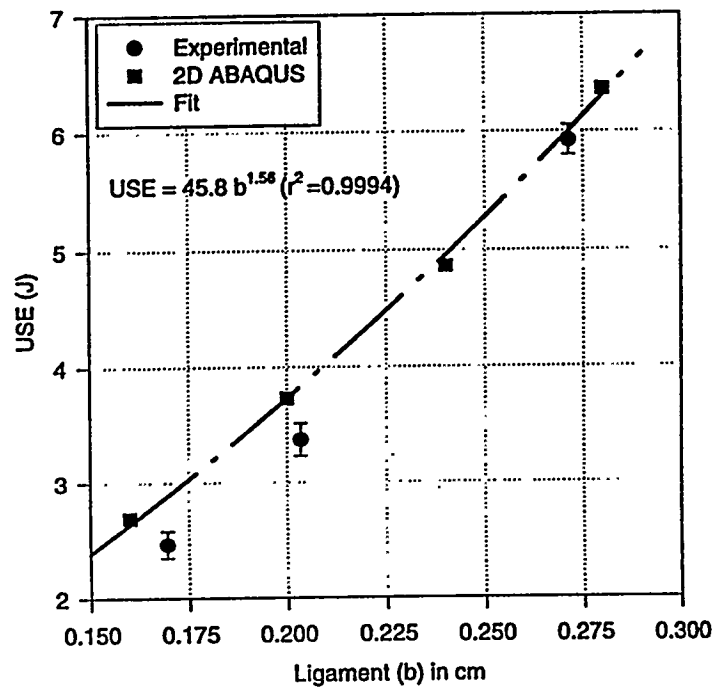


Fig. 8. USE vs. Ligament Size (b) for Medium Size Specimen Medium USE Material

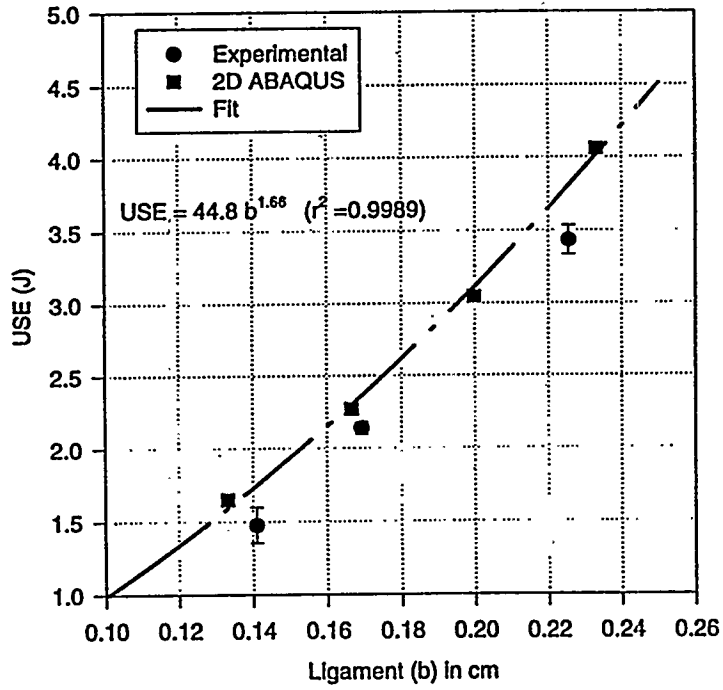


Fig. 9. USE vs. Ligament Size (b) for Third Size Medium USE Material

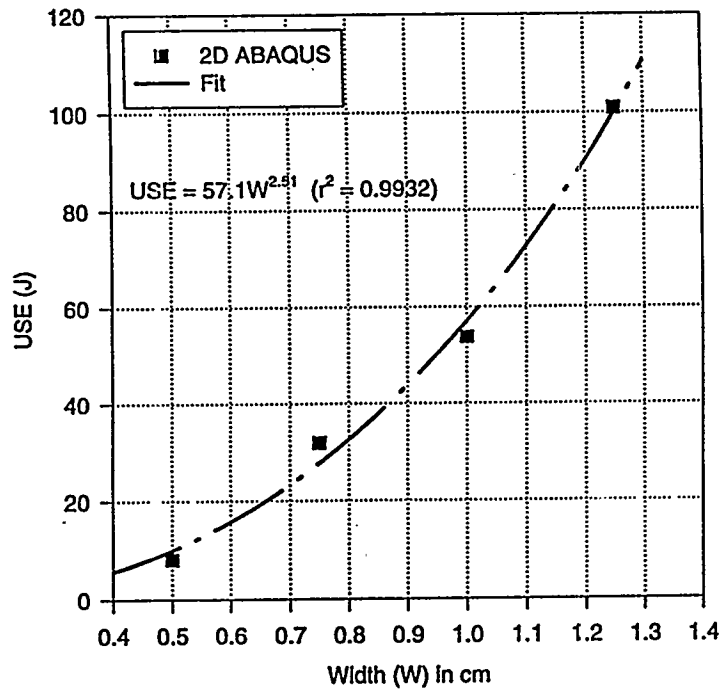


Fig. 10. USE vs. Width (W) for Full Size Medium USE Material 50% W Precracked

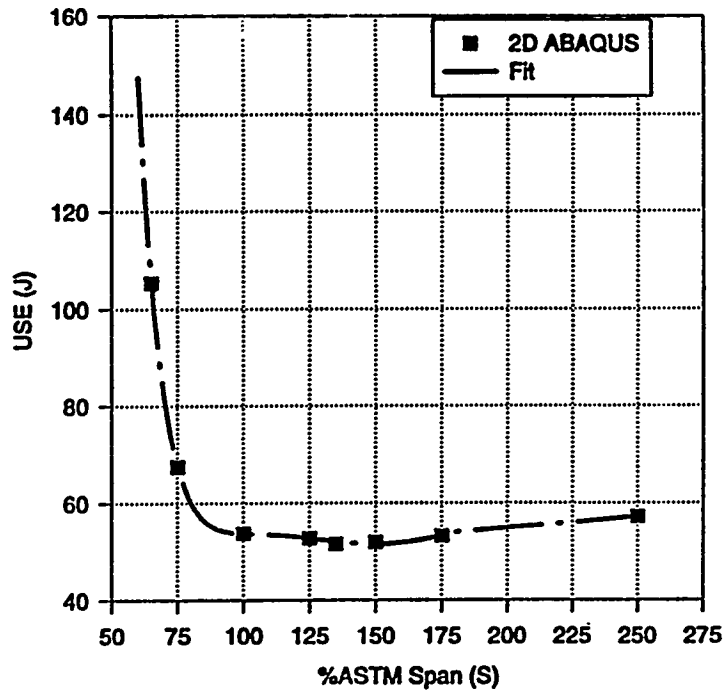


Fig. 11. USE vs. %ASTM Span (S) for Full Size Medium USE 50% W Precrack

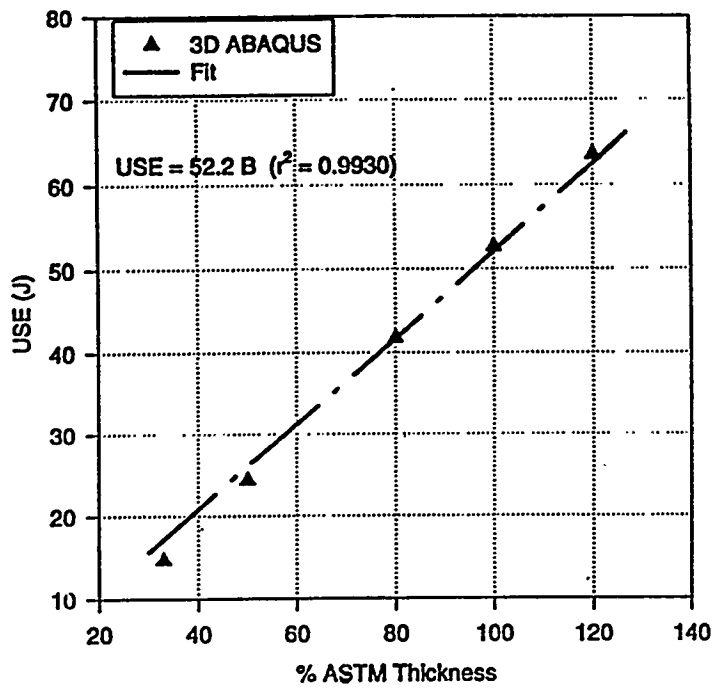


Fig. 12. USE vs. Thickness (B) for 3D Full Size Medium USE Material (Precracked 50% W)

40 to 70% of the width. The  $b$  dependence varied from about  $3/2$  for subsize specimens to 2 for full size specimens.

(3)  $USE_p$  for full size specimens varied with  $W^{2.51}$  and varied linearly with thickness ( $B$ ).  $USE_p$  increased steeply with decreasing span for spans less than 4.000 cm. Little span dependence was observed for spans larger than 4.000 cm.

#### Acknowledgment

This work was supported by the United States Department of Energy under contract DE-AC04-94AL85000 and also DE-AC06-76RLO 1830.

#### References

- [1] W.R. Corwin, R.L. Klueh, and J.M. Vitek, J. Nucl. Mater., Vols. 122 & 123, (1984), p. 343.
- [2] W. R. Corwin and A. M. Hougland, The Use Small Scale Specimens for Testing Irradiated Material, ASTM STP 888, W. R. Corwin and G. E. Lucas, Eds., American Society of Testing and Materials, Philadelphia, 1986, p. 325.
- [3] B. L. Ferguson, American Society for Metals. (ASM) Proceedings of American Institute of Mining, Metallurgical, and Petroleum Engineers, (AIME) Annual Meeting on "What Does the Charpy Test Really Tell Us?," Denver, CO, Feb. 1978, A.R. Rosenfield, et al., Eds., pp. 90-107.
- [4] F. Abe, T. Noda, H. Araki, M. Okada, M. Narai, and H. Kayano, Journal of Nuclear Materials, Vol. 150, 1987, pp. 292-301.
- [5] G. E. Lucas, G. R. Odette, J. W. Shekherd, P. McConnell, and J. Perrin, The Use of Small-Scale Specimens for Testing Irradiated Material, ASTM STP 888, W. R. Corwin and G. E. Lucas, Eds., American Society for Testing and Materials for Testing and Materials, Philadelphia, 1986, p. 305.
- [6] G. E. Lucas, G. R. Odette, J. W. Shekherd, and M. R. Krishnadev, Fusion Technology, Vol. 10, 1986, p. 728.
- [7] B. S. Loudon, A.S. Kumar, F.A. Garner, M.L. Hamilton, and W. L. Hu, J. Nucl. Mater., Vols. 155 to 157, 1988, pp. 662-667.
- [8] A. S. Kumar, F. A. Garner, and M. L. Hamilton, Effects of Radiation on Materials: 14th International Symposium (Volume II), ASTM STP 1046, N. H. Packan, R. E. Stoller, and A. S. Kumar, Eds., American Society for Testing and Materials, Philadelphia, 1990, pp. 487-495.
- [9] S. T. Rosinski, A. S. Kumar, N. S. Cannon, and M. L. Hamilton, ASTM STP 1204, W. R. Corwin, W. L. Server, and F. M. Haggag, Eds., American Society for Testing and Materials, Philadelphia, 1993, pp. 405-416.
- [10] A. S. Kumar, Cannon N. S., S. T. Rosinski, M. L. Hamilton, Effect of Radiation on Materials: 16th International Symposium, ASTM STP 1175, Arvind S. Kumar, David S.

- Gelles, Randy K. Nanstad, and Edward A. Little, Editors, American Society for Testing and Materials, Philadelphia, 1993, pp. 147-155.
- [11] H. Kayano, H. Kurishita, M. Narui, M. Yamazaki, Y. Suzuki, *Journal of Nuclear Materials*, Vols. 179-181, 1991, pp. 425-428.
- [12] D.J. Alexander, and R.L. Klueh, "Specimen Size Effects in Charpy Impact Testing," ASTM STP 1072, John M. Holt, Ed., American Society for Testing & Materials, Philadelphia, 1990, p. 179.
- [13] A.D. Amayev, V.I. Badanin, A.M. Kryukov, V.A. Nikolayev, M.F. Rogov, A. Sokolov, ASTM STP 1204, W. R. Corwin, W. L. Server, and F. M. Haggag, Eds., American Society for Testing and Materials, Philadelphia, 1993, pp. 424-439.
- [14] H. Kurishita, H. Kayano, M. Narui, M. Yamazaki, Y. Kano, I. Shibahara, *Materials Transactions*, Vol. 34, 1993, pp. 1042-1052.
- [15] A. S. Kumar, L.E. Schubert, M. L. Hamilton and N.S. Cannon, *J. Nucl. Mater.*, Vols. 225 (1995)238.
- [16] L.E. Schubert, A. S. Kumar, S.T. Rosinski and M. L. Hamilton, *J. Nucl. Mater.*, Vols. 225 (1995)231.
- [17] H. Kurishita, H. Kayano, M. Narui, M. Yamazaki, *Journal of Nuclear Materials*, Vols. 212-215 (1994) 1682-1687.
- [18] H. Kurishita, H. Kayano, M. Narui, M. Yamazaki, Y. Kano, and I. Shibahara, *Materials Transactions, JIM*, Vol. 34, No. 11 (1993) 1042-1052.
- [19] A. S. Tetelman, *Fracture of Structure Materials*, John Wiley & Sons, Ed., 1967, P. 295.
- [20] Hibbit, Karlsson, & Sorensen, Inc., *ABAQUS Explicit Users Manual Ver. 5.4*, HKS 1995.
- [21] S. E. Sidener, *Dynamic Finite Element Analysis of Charpy Impact Tests for use in Nuclear Power Plant Life Extension*, M.S. Thesis, University of Missouri-Rolla, December 1995.
- [22] *Nuclear Pressure Vessel Steel Data Base*, Electric Power Research Institute Report Number-NP-933, December 1978.
- [23] F.M. Haggag, *In-Situ Measurements of Mechanical Properties Using Novel Automated Ball Indentation System, Small Specimen Test Techniques Applied to Nuclear Reactor Vessel Thermal Annealing and Plant Life Extension*, ASTM STP 1204, W.R. Corwin, F.M. Haggag, and W.L. Server, Eds., American Society for Testing and Materials, Philadelphia, 1993, pp. 27-44.